

**ANALYSIS OF INTERACTION BETWEEN A
CRYSTALLOGRAPHICALLY UNIAXIAL FERRITE
RESONATOR AND A HALL-EFFECT TRANSDUCER**

M. Y. Koledintseva

University of Missouri-Rolla
Rolla, MO 65409, USA

A. A. Kitaitsev

Ferrite Laboratory of Moscow Power Engineering Institute
(Technical University)
Krasnokazarmennaya, 14, Moscow 111250, Russia

Abstract—In this paper, a number of physical phenomena taking place at the interaction of a crystallographically uniaxial ferrite resonator (UFR) with a semiconductor element, such as a Hall-effect transducer (HET), are analyzed. The UFR in this study is in a direct contact with an unpackaged HET. The interaction is studied in the vicinity of the ferromagnetic resonance in the UFR. The analytical model based on the combination of the problem of interaction of an arbitrarily orientated and shaped UFR with electromagnetic field of a multimode transmission line (waveguide) and thermal balance equations is proposed. A number of thermo/electro/magnetic phenomena that cause a voltage additional to that of the Hall-effect in the HET are analyzed. It is shown that this additional voltage is mainly due to Nernst-Ettingshausen thermo-magnetic effect. Some experimental results in 8-mm waveband are presented. This structure may serve as a frequency-selective primary transducer for detection and measurement of microwave (or millimeter-wave) power.

1. INTRODUCTION

Ferrite resonators (FR) have a long history of applications in microwave engineering as frequency-selective elements of filters, circulators, power and frequency converters, resonance detectors, cross-multipliers, etc. They are widely used in various devices for microwave frequency-selective measurements, such as spectrum analyzers, measurers of spectral power density, and peak power meters [1, 2]. Their operation typically requires very intense magnetization fields, especially as the operating frequencies increase to the extremely high frequency (EHF) band and above, and this is a shortcoming of ferrite applications. However, the present-day high-quality resonators made of crystallographically uniaxial ferrites, such as monocrystalline hexagonal ferrites, do not require huge magnetic systems for achieving ferromagnetic resonance, since they have high internal field of magnetic crystallographic anisotropy [1–3].

It is known that a high-quality ferrite resonator, i.e., with a narrow line of ferromagnetic resonance (FMR), effectively picks out energy from electromagnetic field at the ferromagnetic resonance. Thus the typical linewidth of FMR for monocrystalline barium hexagonal ferrites is on the order of a few dozen oersteds ($10 \dots 30$ Oe), which corresponds to about $30 \dots 100$ MHz. As for monocrystalline garnet ferrites, modern technology allows for obtaining resonators with a resonance linewidth as low as a few millioersteds, or $0.1 \dots 1$ MHz. If the Q-factor of a FR were infinitely large, this energy at the resonance frequency would be stored in the FR forever. But in reality, Q-factor is never infinite, and the accumulated energy partially re-radiates, and partially dissipates within the FR body, eventually producing heat. Both re-radiated energy and heat loss in the FR depend on coupling between the FR and the electromagnetic field. This coupling, in turn, depends on physical properties of the ferrite material, geometry of the resonator, as well as on the intensity, frequency, and the mode structure of the incident electromagnetic field.

Many years ago in [4], the idea of the yttrium-iron garnet (YIG) ferrite bolometer was proposed. This is a ferrite element in a direct thermal contact with a semiconductor element. At the ferromagnetic resonance, the ferrite resonator heats up, and the resistance of the semiconductor element varies. This variation tells about the intensity of the electromagnetic field. However, this idea has not found practical application, because a YIG ferrite needed huge magnetic system for its operation at the FMR, and at the same time sensitivity and dynamic range of such a bolometer were very low. Actually, the narrower linewidth of a YIG resonator, the higher frequency selectivity and

resolution it provides. However, an extremely high Q-factor is in a conflict with heating of a ferrite resonator. Hence, there should be an optimum linewidth of FMR in a ferrite resonator to satisfy both frequency selectivity and sensitivity, as well as a high conversion coefficient of a ferrite bolometer.

In our work [5], it was experimentally shown that it is possible to use the structure based on the hexagonal ferrite resonator and a semiconductor element for frequency-selective power detection in the frequency range around 40 GHz without a massive external magnetic system. The interaction was experimentally detected in the vicinity of the ferromagnetic resonance, and only a low-intensity bias magnetic field for saturation of the hexagonal ferrite and the FMR tuning was needed. Barium hexagonal ferrites typically have wider resonance linewidths than garnet ferrites, and this is preferable from the point of view of their enhanced heating by microwaves (mm-waves) in the vicinity of the FMR.

The objectives of this paper are (1) to analyze the main physical phenomena that take place at the interaction of the uniaxial ferrite resonator (UFR) with a particular semiconductor element — an unpackaged Hall-effect transducer (HET), and (2) to develop a generalized analytical (electromagnetic plus thermal) model for the power conversion coefficient in this structure.

Figure 1 contains the classification of the possible physical mechanisms of interaction between a UFR and a semiconductor element at frequencies close to the FMR. These mechanisms can be divided into two groups: (1) low-inertial (electromagnetic) and (2) inertial (thermal). Practically, low-inertial electromagnetic mechanisms allow for measuring power parameters of pulse signals, while inertial thermal mechanisms would be useful only for measuring power parameters of continuous signals or average power of pulses at the resonance frequency of the UFR.

Low-inertial effects are related to variations of the magnetization vector of an UFR. These variations are expected to be noticeable at comparatively high power levels (e.g., more than 1 W), depending on the level of useful variations of voltages induced in the semiconductor elements and sensitivity of voltmeters used to detect these variations. Besides, at comparatively low microwave power levels (below 1 W), low-inertial effects are masked by thermal phenomena, and, mainly, microwave power is converted to a d.c. voltage.

Inertial, or thermal, mechanism of interaction appears as a heat transfer from the UFR to a thermo-sensitive semiconductor element. The electromagnetic power absorbed by the UFR at the FMR converts to heat, and the heat flux penetrates through the body of the

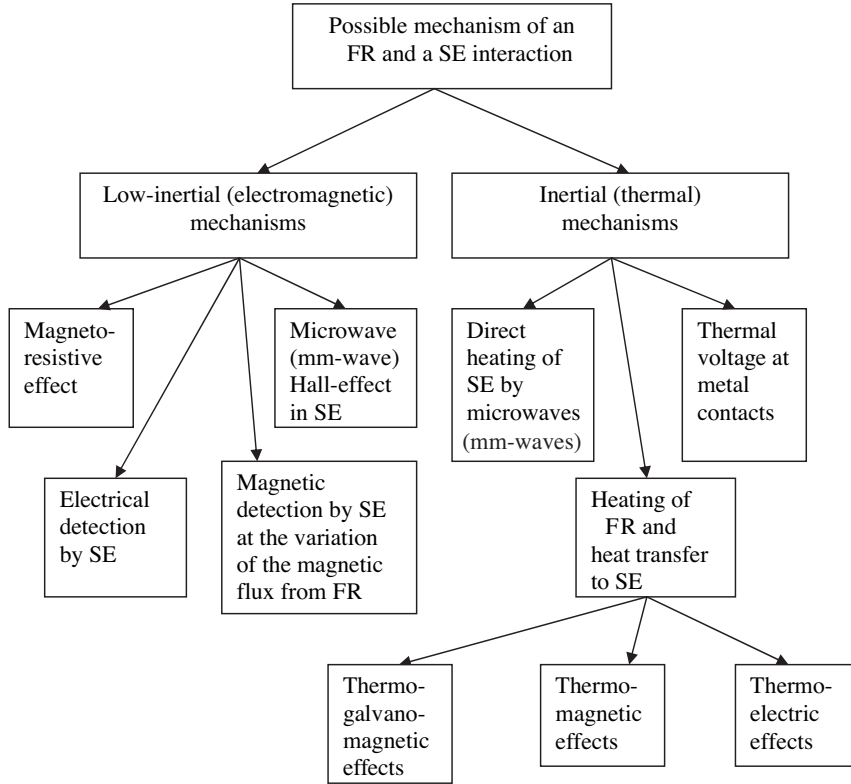


Figure 1. Schematic of possible mechanisms of interaction between an FR and a semiconductor element (SE) at mm-wave frequencies close to FMR.

semiconductor element. If this semiconductor element is a Hall-effect transducer, it operates at some bias d.c. current flowing through it between two opposite contacts. Together with the UFR, it is placed in a bias magnetic field, needed for achieving FMR in the UFR. Along with the Hall-effect, there is a number of thermoelectric, thermomagnetic, galvanomagnetic, and thermoelectromagnetic phenomena. Overall, there are known over 560 different effects accompanying the Hall-effect [6], and they may cause voltage in the HET additional to that of the Hall-effect.

The structure of the paper is the following. Some results of computations based on the proposed analytical model are provided in Section 2. Section 3 describes some experimental results. Conclusions are summarized in Section 4.

2. ANALYTICAL MODEL

Recently an interest to analysis of temperature inside objects due to electromagnetic power impact has increased [7]. Problems of this kind arise, for example, when quantifying effects of RF, microwave, or mm-wave heating of biological tissues, or at thermal modeling for optimization of heating processes in microwave ovens [8]. Such problems are typically solved through the energy conservation law, or heat-transfer equation.

This Section contains an analytical model for the conversion of microwave power to a d.c. voltage that appears on the contacts of a Hall-effect transducer due to the direct contact with a uniaxial ferrite resonator. The analytical model includes both interaction of the UFR with the electromagnetic field and thermal balance in the system.

Let us consider the case when a microwave oscillation of the power $P(f_0)$ acts on the UFR continuously, and the UFR absorbs this power due to the FMR. Inside the UFR there is a constant source of heat, and the surface temperature of the UFR remains constant. Suppose that heat radiation is absent. Let us also neglect heating of a semiconductor when current flows in it, and assume that there is no difference in the temperature of the contacts (no thermal electromotive force). The result of the semiconductor heating is the variation in the charge carrier mobility, which leads to the variation of its thermal coefficient K_T . The latter relates the useful induced voltage and the temperature variation of the HET as

$$\Delta V = K_T \Delta T. \quad (1)$$

If the stationary regime is considered,

$$\Delta T = \Delta T_{stat} = T_{stat} - T_0, \quad (2)$$

where T_0 is the initial temperature of the HET, and T_{stat} is the stationary temperature in the system. In the stationary regime, the maximum useful induced voltage $\Delta V = \Delta V_{max}$ is achieved.

The conversion coefficient of the system UFR-HET can be defined as a ratio of the maximum useful induced voltage to the power of an input microwave signal at the given frequency [1],

$$K_p = \Delta V_{max} / P(f_0), \quad (3)$$

or

$$K_p = K_T \Delta T_{stat} / P(f_0), \quad (4)$$

Assume that the thermal coefficient K_T of HET is known, and the power $P(f_0)$ is also known (can be measured). To find the conversion coefficient K_p , it is necessary to calculate the temperature increase ΔT_{stat} , which depends on the power absorbed by the UFR at the FMR,

$$P_{abs} = \alpha_{abs} P(f_0), \quad (5)$$

where α_{abs} is the absorption coefficient. The absorption coefficient depends on the UFR coupling with the transmission line where it is placed. The corresponding coupling coefficient η_c is a function of many factors: the geometry of the transmission line, the operating mode structure, the point where the UFR is situated, physical parameters of the UFR (namely, its resonance line width ΔH , saturation magnetization M_S , anisotropy field H_A , and orientation of the HFR crystallographic axis in respect with the bias magnetic field H_0), as well as the detuning $a = |f_{res} - f_0|/f_0$ of the FMR frequency from the microwave signal carrier frequency.

The absorption coefficient can be obtained through solving an electromagnetic power balance equation and using a *self-matched field* approach, as described in [1, 9]. From this analysis, the absorption coefficient α_{abs} relates to the coupling coefficient η_c as

$$\alpha_{abs} = 2|\eta_c|/|1 + \eta_c|. \quad (6)$$

The general formula for the coupling coefficient of the ferrite resonator with a multimode transmission line or a waveguide can be obtained using the formulation in [10], and can be written as

$$\eta_c = \det \left\{ \overleftrightarrow{T} + j \overleftrightarrow{\chi}_{xyz} \overleftrightarrow{w} \right\} - 1, \quad (7)$$

where \overleftrightarrow{T} is the unity tensor, \overleftrightarrow{w} is the coupling matrix [11]

$$\overleftrightarrow{w} = \frac{\omega \mu_0 V_f}{2} \begin{bmatrix} \sum_{n=1}^N \frac{h_{xn}^+ h_{xn}^-}{\tilde{P}_n} & \sum_{n=1}^N \frac{h_{yn}^+ h_{xn}^-}{\tilde{P}_n} & \sum_{n=1}^N \frac{h_{zn}^+ h_{xn}^-}{\tilde{P}_n} \\ \sum_{n=1}^N \frac{h_{xn}^+ h_{yn}^-}{\tilde{P}_n} & \sum_{n=1}^N \frac{h_{yn}^+ h_{yn}^-}{\tilde{P}_n} & \sum_{n=1}^N \frac{h_{zn}^+ h_{yn}^-}{\tilde{P}_n} \\ \sum_{n=1}^N \frac{h_{xn}^+ h_{zn}^-}{\tilde{P}_n} & \sum_{n=1}^N \frac{h_{yn}^+ h_{zn}^-}{\tilde{P}_n} & \sum_{n=1}^N \frac{h_{zn}^+ h_{zn}^-}{\tilde{P}_n} \end{bmatrix}, \quad (8)$$

where N is the number of modes, V_f is the volume of the ferrite resonator, and pluses and minuses stand for the forward and backward

directions of the mode propagation. The norm of the corresponding n -th transmission line or waveguide mode is calculated through the vector product of the phasor of electric field and the complex-conjugated magnetic field phasor of the corresponding mode [12, 13]

$$\tilde{P}_n = -2 \int_{S_{cross}} [\vec{e}_n \times \vec{h}_n^*] \cdot d\vec{s}, \quad (9)$$

where index n might stand for two numbers, e.g., “10” in the notation of the TE₁₀ waveguide mode.

Assume that a monocrystalline uniaxial ferrite with the crystallographic axis $c \parallel \vec{H}_A$ is magnetized up to saturation by the bias magnetic field $\vec{H}_0 \parallel \hat{z}$, as is shown in Figure 2. The direction of the equilibrium magnetization \vec{M}_0 is determined by the angles φ and θ with respect to the axes x and z , correspondingly.

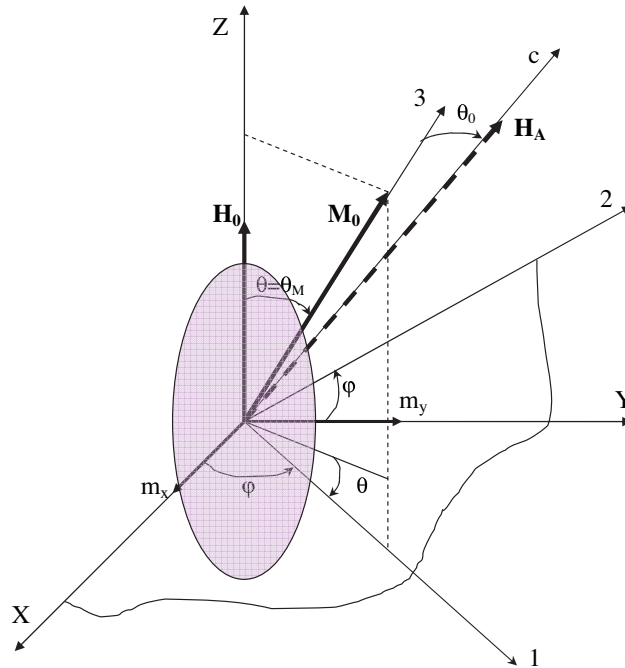


Figure 2. Orientation of the vectors describing magnetic susceptibility tensor of a uniaxial monocrystalline ferrite resonator.

In the Cartesian coordinate system $\{\hat{x}, \hat{y}, \hat{z}\}$, the susceptibility tensor of a crystallographically anisotropic UFR at an arbitrary

orientation of its axis of magnetic anisotropy with respect to the bias magnetic field is a 9-component tensor

$$\overleftarrow{\chi}_{xyz} = \begin{vmatrix} \chi_{xx} & \chi_{xy} & \chi_{xz} \\ \chi_{yx} & \chi_{yy} & \chi_{yz} \\ \chi_{zx} & \chi_{zy} & \chi_{zz} \end{vmatrix}. \quad (10)$$

The components of the external tensor $\overleftarrow{\chi}_{xyz}$ are obtained by the double transform (rotation on the angle θ and on the angle φ) of the susceptibility tensor $\overleftarrow{\chi}_{123}$. The latter is written in the coordinate system $\{\hat{1}, \hat{2}, \hat{3}\}$, tied to the direction of the equilibrium magnetization $\vec{M}_0 \parallel \hat{3}$, and its components are

$$\vec{\chi}_{123} = \begin{vmatrix} \chi_{11} & j\chi_a & 0 \\ -j\chi_a & \chi_{22} & 0 \\ 0 & 0 & 0 \end{vmatrix}. \quad (11)$$

Then the elements of the tensor $\overleftarrow{\chi}_{xyz}$ are calculated through the elements of the tensor $\overleftarrow{\chi}_{123}$ as

$$\begin{aligned} \chi_{xx} &= \chi_{11} \sin^2 \varphi + \chi_{22} \cos^2 \varphi \cos^2 \theta; \\ \chi_{yy} &= \chi_{11} \cos^2 \varphi + \chi_{22} \sin^2 \varphi \cos^2 \theta; \\ \chi_{xy} &= \frac{1}{2} (\chi_{22} \cos^2 \theta - \chi_{11}) \sin 2\varphi + j\chi_a \cos \theta; \\ \chi_{yx} &= \frac{1}{2} (\chi_{22} \cos^2 \theta - \chi_{11}) \sin 2\varphi - j\chi_a \cos \theta; \\ \chi_{zx} &= -\frac{1}{2} \chi_{11} \sin 2\theta \cos \varphi + j\chi_a \sin \theta \sin \varphi; \\ \chi_{xz} &= -\frac{1}{2} \chi_{11} \sin 2\theta \cos \varphi - j\chi_a \sin \theta \sin \varphi; \\ \chi_{zy} &= -\frac{1}{2} \chi_{11} \sin 2\theta \sin \varphi + j\chi_a \sin \theta \cos \varphi; \\ \chi_{yz} &= -\frac{1}{2} \chi_{11} \sin 2\theta \sin \varphi - j\chi_a \sin \theta \cos \varphi; \\ \chi_{zz} &= \chi_{11} \sin^2 \theta, \end{aligned} \quad (12)$$

The parameters of the tensor (11) for the UFR of an arbitrary shape and orientation of the main crystallographic axis can be written based on [10] as

$$\chi_{11} = \frac{\omega_M \omega_1 + j\omega \omega_M \alpha_{LL}}{\omega_1 \omega_2 - \omega^2 (\alpha_{LL}^2 + 1) + j\omega \alpha_{LL} (\omega_1 + \omega_2)};$$

$$\begin{aligned}\chi_{22} &= \frac{\omega_M \omega_2 + j\omega \alpha_{LL}}{\omega_1 \omega_2 - \omega^2 (\alpha_{LL}^2 + 1) + j\omega \alpha_{LL} (\omega_1 + \omega_2)}; \\ \chi_a &= \frac{\omega_M \omega}{\omega_1 \omega_2 - \omega^2 (\alpha_{LL}^2 + 1) + j\omega \alpha_{LL} (\omega_1 + \omega_2)};\end{aligned}\quad (13)$$

$$\begin{aligned}\omega_1 &= \omega_{10} \cos \theta_M + \omega_A \cos^2 \theta_0; & \omega_2 &= \omega_{20} \cos \theta_M + \omega_A \cos 2\theta_0; \\ \omega_{10} &= \omega_0 + \omega_M (N_{22} - N_{33}); & \omega_{20} &= \omega_0 + \omega_M (N_{11} - N_{33}),\end{aligned}$$

where $\omega_0 = \mu_0 \gamma H_0$ is the angular frequency corresponding to the bias magnetic field; $\omega_M = \mu_0 \gamma M_0$ is the angular frequency associated with the magnetization of saturation; $\omega_A = \mu_0 \gamma H_A$ is the angular frequency associated with the field of crystallographic anisotropy; N_{11}, N_{22} and N_{33} are the demagnetization form factors corresponding to the axes $\hat{1}, \hat{2}$ and $\hat{3}$, respectively. A UFR can be of an arbitrary ellipsoid with form factors calculated similarly to depolarization form factors of a dielectric ellipsoid in [14, 15], and the sum of the form factors $N_{11} + N_{22} + N_{33}$ should always be equal to 1. If the UFR is a sphere, then $\omega_{10} = \omega_{20} = \omega_0$.

The parameter α_{LL} is the Landau-Lifshitz dissipation factor, which turns into the Bloch dissipative term, if $\alpha_{LL} = \chi_0 \omega_r / \omega_M$ [10], and can be used for describing ferromagnetic resonance in a uniaxial ferrite. The parameter χ_0 is the static magnetic susceptibility, and ω_r is the relaxation frequency of the UFR. The permeability of vacuum is $\mu_0 = 4\pi \cdot 10^{-7}$ H/m, and the gyromagnetic ratio is $\gamma = 1.76 \cdot 10^{11}$ C/kg. In (10), $\theta_M = \theta$ is the angle between the axis z and equilibrium magnetization direction $\vec{M}_0 \parallel \hat{3}$, and θ_0 is the angle between $\vec{M}_0 \parallel \hat{3}$ and the UFR crystallographic axis $\vec{c} \parallel \vec{H}_A$. The angle θ_0 is calculated from the \vec{M}_0 equilibrium, following from the minimum of the magnetic energy of the crystal, $\theta = \arcsin(H_A \sin 2\theta_0 / 2H_0)$ [10, 13].

After deriving the absorbed power P_{abs} through the electromagnetic parameters of the UFR and the transmission line, where it is placed, let us consider the equation of the thermal balance in the system UFR-HET,

$$P_{abs} = P_{FH} + P_{HM} + P_{FA} + P_{HA}. \quad (14)$$

In (14), P_{FH} is the heat power transferred by the ferrite to the HET (conduction heat exchange); P_{HM} is the heat power transferred from the HET to the metal contacts (also conduction heat exchange); P_{FA} is the heat power transferred by the HFR surface to air (convection heat exchange); and P_{HA} is the heat power given to air by the semiconductor (convection heat exchange).

This power (thermal) balance equation can be re-written as the ordinary linear differential equation with a non-zero right-hand part,

corresponding to the heat source associated with the UFR at FMR, analogous to that for a YIG bolometer in [4]

$$C_{\Sigma} \frac{dT}{dt} + \Psi_{T\Sigma} T = P_{abs}, \quad (15)$$

where C_{Σ} [J/K] is the total heat capacity of all the elements of the thermal system, and $\Psi_{T\Sigma}$ [W/K] is the total heat-transfer factor of all the system. This equation describes the transient thermal regime in the system UFR-HET. The initial condition for temperature increase $T(t)$ is

$$T(0) = T_0 \quad (16)$$

where T_0 is the surrounding (room) temperature. The solution of the Cauchy problem (15)–(16) is an exponential function

$$T(t) = T_0 + \Delta T_{stat}(1 - e^{-t/\tau_{\Sigma}}). \quad (17)$$

The increase up to the stationary temperature is calculated as

$$\Delta T_{stat} = P_{abs}/\Psi_{T\Sigma}, \quad (18)$$

and the system response time is

$$\tau_{\Sigma} = C_{\Sigma}/\Psi_{T\Sigma}. \quad (19)$$

Let us consider two cases.

- 1) *The microwave signal is far from the FMR in the UFR.* There is no resonance absorption in the UFR, and the UFR is almost not heated up by microwaves (ε'' associated with conductivity currents in the ferrite resonator is extremely low, and μ'' associated with the loss at spin resonance is very low outside the FMR, too). There is only the Hall-effect voltage in the HET, since the HET is placed in the bias magnetic field together with the UFR.
- 2) *The frequency of the microwave signal falls within the FMR line.* The UFR heats up due to microwave power absorption and high resonance value of μ'' . In addition to the Hall-effect voltage, the heat-related voltage is induced on the contacts of the HET that directly touches the UFR. The magnitude of this additional voltage is proportional (with the coefficient K_P) to the average power of the microwave signal at the resonance frequency of the UFR, according to (3),

$$\Delta V_{\max} = K_p P_{av}(f_{res}). \quad (20)$$

In the experiments the structures may be exposed to microwave pulses with some pulse repetition frequency and an off-duty factor. For this reason, in (20), $P_{av}(f_{res})$ is the average microwave power at the FMR frequency. Low-inertial effects, such as the magneto-resistive effect, the microwave Hall-effect in semiconductor, the direct electromagnetic field detection by HET, and the magnetic detection by HET due to variation of magnetic flux from the UFR in the general case also present. However, as our further studies have shown, they are negligibly small at the average power levels of a few dozens microwatt. The mechanism of the voltage induced in the HET at the UFR-HET structure interaction with microwaves is of the inertial thermal nature, and is determined by heating of the UFR at the FMR and the corresponding heat flux acting on the HET.

Suppose that the total voltage induced in a semiconductor plate with current I in the transverse magnetic field H_{0z} contains the Hall-effect voltage V_H and a number of additional terms, corresponding to the most important effects accompanying the Hall-effect [6],

$$V = V_H + V_{neq} + V_{mr} + V_{temf} + V_E + V_{NE} + V_{PNE} + V_{RL} + V_{PRL}. \quad (21)$$

In (21), V_{neq} is the non-equipotentiality voltage; V_{mr} is the magneto-resistive voltage; V_{temf} is the thermoelectromotive force voltage; V_E is the Ettingshausen galvano-thermo-magnetic voltage; V_{NE} is the Nernst-Ettingshausen thermo-magnetic voltage; V_{PNE} is the Peltier-Nernst-Ettingshausen thermo-magnetic electrothermal/thermo-galvano-magnetic voltage; V_{RL} is the Righi-Leduc thermo-magnetic voltage; and V_{PRL} is the Peltier-Righi-Leduc electrothermal and thermo-galvano-magnetic voltage.

The contributions of V_H and V_{mr} may be compensated by using the second Hall-element, placed in the same bias magnetic field, but not in a direct thermal contact with the UFR. As for the voltages V_{neqv} and V_{temf} , they are independent of the bias magnetic field, and can be taken into account and compensated, too. Then the magnitude of the useful increase of the voltage that will be later measured is comprised of the rest five contributions:

$$\Delta V_{\max} = V_E + V_{NE} + V_{PNE} + V_{RL} + V_{PRL}. \quad (22)$$

These five effects, acting upon the voltage in the structure UFR-HET are summarized in Table. In practice, it is very difficult (if not impossible) to separate these five contributions. It is assumed that the bias magnetic field is in the z -direction and the operation current in

Table 1. Effects acting of voltage in UFR-HET structure.

Notation	Name of the voltage	Type of the effect	Dependence of voltage on	Symbolic
V_E	Ettingshausen	Galvano-thermo-magnetic	Direction of current, magnetic field, sign of charge carriers	$(I_y, H_z) \rightarrow \frac{\partial T}{\partial x} \rightarrow V_x$
V_{NE}	Nernst-Ettingshausen	Thermo-magnetic	Direction of magnetic field, sign of charge carriers	$(\frac{\partial T}{\partial y}, H_z) \rightarrow V_x, V_y$
V_{PNE}	Peltier-Nernst-Ettingshausen	Thermo-magnetic electrothermal and thermo-galvano-magnetic	Direction of current, magnetic field, sign of charge carriers	$(I_y \rightarrow \frac{\partial T}{\partial y}, H_z) \rightarrow V_x, V_y$
V_{RL}	Righi-Leduc	Thermo-magnetic	Direction of magnetic field	$(\frac{\partial T}{\partial y}, H_z) \rightarrow \frac{\partial T}{\partial x} \rightarrow V_x$
V_{PRL}	Peltier-Righi-Leduc	electrothermal/thermo-galvano-magnetic	Direction of current and magnetic field	$(I_y \rightarrow \frac{\partial T}{\partial y}, H_z) \rightarrow \frac{\partial T}{\partial x} \rightarrow V_x$

the HET flows in the y -direction. It is shown symbolically in Table 1 what the primary values or components are, what effects they cause, and what voltage components they produce.

However, it is reasonable to speculate that the voltage V_{NE} due to the Nernst-Ettingshausen effect might be dominating. The reasoning for this is that this effect belongs to the thermo-magnetic effects and appears as a transverse voltage with respect to the current I flowing in the semiconductor slab, if the latter is affected by a magnetic field and a heat flux simultaneously. This is the case in the structure under study. Therefore, we may conclude that in the structure UFR — Hall-effect transducer, the *frequency-selective Nernst-Ettingshausen effect* is observed.

3. EXPERIMENTAL RESULTS AND COMPUTATIONS BASED ON THE PROPOSED ANALYTICAL MODEL

A UFR made of a monocrystalline M-type Barium hexagonal ferrite doped with Ti and Zn ions ($\text{BaFe}_{9.8}\text{Ti}_{1.1}\text{Zn}_{1.1}\text{O}_{19}$) was placed in a metal rectangular waveguide of a cross-section $7.2 \text{ mm} \times 3.4 \text{ mm}$. The point of a right circularly polarized mm-wave magnetic field was chosen, since it is the point where coupling between the UFR and the TE_{10} mode is the most intense. The UFR was a spheroid with the major

and minor axes of 0.585 mm and 0.557 mm, respectively. Its field of crystallographic magnetic anisotropy was $H_A = 11.3 \text{ kOe}$, and the unloaded resonance line width was $\Delta H = 31.1 \text{ Oe}$. (Herein, the units of Gaussian system are used, as the most widely used among magnetologists. The conversion is $1 \text{ Oe} = 1.2566 \cdot 10^{-2} \text{ A/m}$). The measured input average power of the mm-wave continuous signal at the frequency $f_0 = 39.5 \text{ GHz}$ was $P(f_0) = 60 \text{ mW}$ (the duty-off factor was equal to 2, and the nanosecond pulse repetition frequency was 1 kHz). The UFR absorbed 5 dB at the FMR ($P_{abs}^{meas} = 41.1 \text{ mW}$).

The Hall-effect transducer *X511* (made in Russia) had the size $1.5 \text{ mm} \times 2.0 \text{ mm} \times 0.1 \text{ mm}$. It was made of a monocrystalline InSb, whose thermal coefficient of voltage was $K_T = 1.5 \text{ mV/K}$ (according to the technical passport of *X511*). An active region of contact with the UFR was around 0.01 mm^2 . The heat transfer coefficients at natural convection (room temperature $T_0 = 20^\circ\text{C}$ and normal atmosphere pressure of 760 mm of mercury) for both UFR and HET are about $30 \text{ W}/(\text{m}^2 \cdot \text{K})$.

First, the computations based on the analytical model above were done. In the computations, it was assumed that the density of the hexagonal ferrite was $\rho_f = 4900 \text{ kg/m}^3$, the specific heat was $c_f = 1100 \text{ J}/(\text{kg} \cdot \text{K})$, and thermal conductivity was $\lambda_f = 4.1 \text{ W}/(\text{m} \cdot \text{K})$. The density of InSb was taken as $\rho_s = 5770 \text{ kg/m}^3$, the specific heat was $c_s = 700 \text{ J}/(\text{kg} \cdot \text{K})$, and the thermal conductivity was $\lambda_s = 18 \text{ W}/(\text{m} \cdot \text{K})$.

Based on this data, the calculated total heat transfer factor is $\Psi_{T\Sigma} = \Psi_{conv} + \Psi_{cond} = 1.2 \cdot 10^{-3} \text{ W/K}$, and the total heat capacity is $C_\Sigma = C_f + C_s = 0.9 \cdot 10^{-3} \text{ J/K}$. The calculated response time of the system is $\tau_s = 750 \text{ ms}$, and the calculated stationary temperature increase in the system is $\Delta T_{stat} = 25^\circ\text{C}$. The transition time for the temperature increase is $t_{stat} = 4.6 \cdot \tau_\Sigma = 3.45 \text{ s}$. The calculated maximum HET voltage is $\Delta V_{max} = 37.5 \text{ mV}$, and the corresponding conversion coefficient is $K_p^{calc} = 0.625 \text{ V/W}$. At the same time, the measured data are $\Delta T_{stat}^{meas} = 21^\circ\text{C}$ and $\tau_\Sigma^{meas} \approx 1 \text{ s}$. The calculated and measured temperature increase curves are shown in Figure 4.

In the experiment, two Hall-effect transducers were used: (1) *X511* with $R_{in} = 2.0 \text{ Ohms}$; $R_{out} = 1.6 \text{ Ohms}$; $I_{max} = 100 \text{ mA}$; sensitivity = $1.05 \text{ V}/(\text{A(T)})$, and (2) *X211* with $R_{in} = 2.0 \text{ Ohms}$; $R_{out} = 1.9 \text{ Ohms}$; $I_{max} = 100 \text{ mA}$; sensitivity = $1.38 \text{ V}/(\text{A(T)})$. The first HET *X511* was directly contacting the UFR, and the second HET *X211* was outside the waveguide in a point with the same bias magnetic field for Hall-effect and magnetoresistive effect compensation. The voltage-field slope $S = \Delta V/\Delta H = 10^{-2} \text{ mV/Oe}$ was the same for both Hall elements. The magnetic sensitivity (the minimum measured magnetic field) for

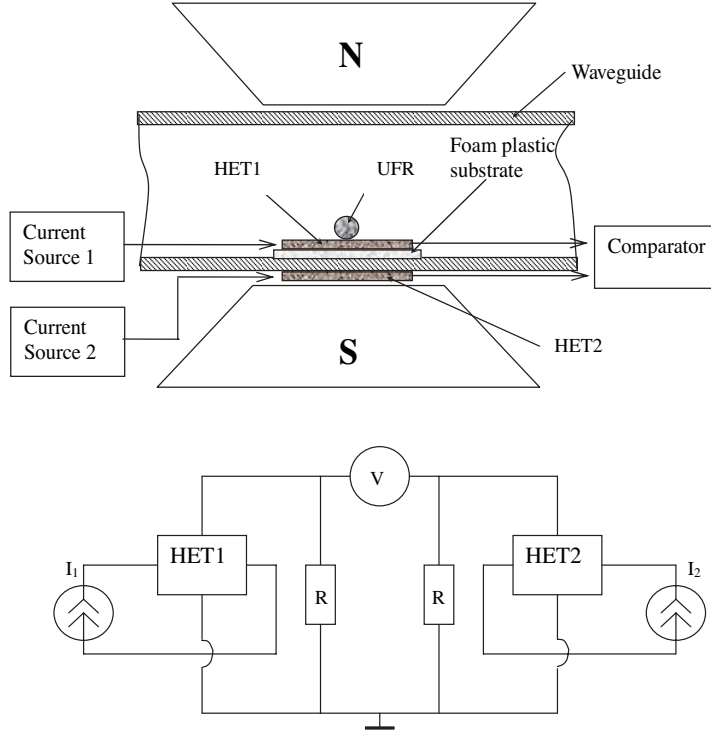


Figure 3. Schematic of the transducer based on the UFR and two Hall- effect transducers.

both HET was 0.1 Oe. The identity of operation of the Hall elements was assured by proper choosing of their operation currents.

The UFR together with the first HET was placed in the point of circular polarization of mm-wave magnetic field of the rectangular waveguide with cross-section $7.2 \text{ mm} \times 3.4 \text{ mm}$. The measured off-resonance loss factor in the section was 1.1 dB, and the standing wave ratio in this section was $\text{SWR} = 1.2$. The UFR was the same as discussed above. The FMR absorption was 5 dB. The dash line in Figure 5 shows the resonance dependence of the differential signal ΔV_{max} as a function of the applied bias magnetic field H_{z0} for the transducer based on the structure UFR-HET. For this curve, the microwave signal was continuous at the frequency $f_0 = 40.7 \text{ GHz}$, and the average power of the signal was 60 mW. The minimum stable measured signal was about $10 \mu\text{W}$. The conversion coefficient was $K_P^{\text{meas}} = 0.6 \text{ V/W}$, which is slightly smaller than the calculated value ($K_P^{\text{calc}} = 0.625 \text{ V/W}$). The discrepancy can be explained by the

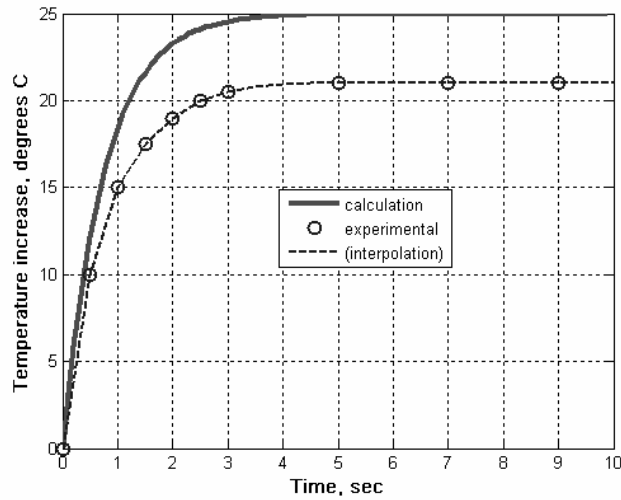


Figure 4. Temperature increase in the structure UFR — Hall element at the FMR absorption by the UFR.

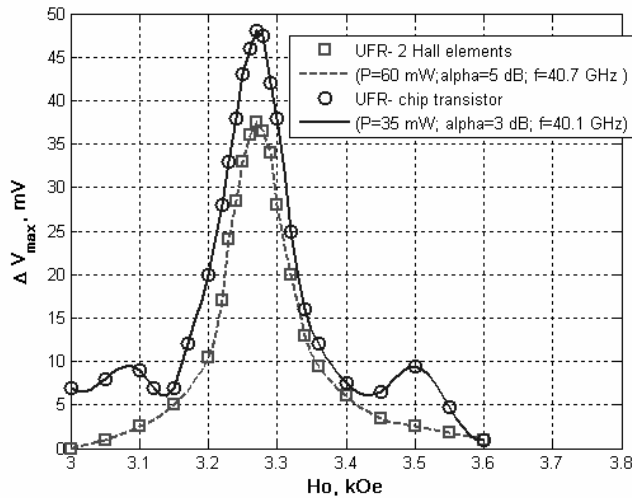


Figure 5. Resonance dependence of the converted voltage.

microwave loss in the section of the waveguide. Besides, the UFR loaded Q -factor decreased compared to the unloaded one not only because of the coupling with the waveguide, but also because the UFR was loaded with the semiconductor element. The 50% alcohol

solution of the commercially available glue *BF-2* (Russia) was used to fix the UFR on the unpackaged HET, and the resonance absorption in a high- Q ferrite resonator could decrease by 1–2 dB. The simplified assumptions in the model, for example, neglect of heat loss on metal contacts, might also influence accuracy of computations, as well as the numerical data on the parameters of a transmission line, ferrite resonator, and InSb HET assumed for the model might have some discrepancy with the real numbers. Besides, instrumental error at the microwave measurements might yield another 1 dB.

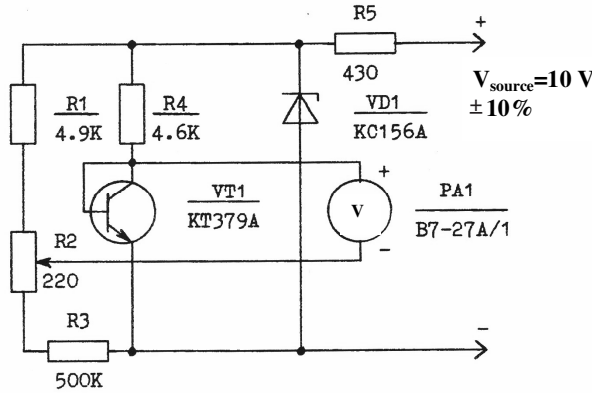


Figure 6. Schematic of the chip transistor thermosensor touching the UFR.

In another experiment, the internal HET contacting with the UFR was substituted by another semiconductor thermosensitive element, which was an unpackaged chip transistor (CT), used as a diode (directly connected base and collector, as shown in Figure 6). The thermal sensitivity of the CT of the type *2TC398A-1* (Russia) was 3.0 mV/K, which is higher than that of the HET. The monocrystalline uniaxial hexagonal ferrite resonator used in this experiment had an anisotropy field $H_A = 10.6$ kOe, unloaded resonance line $\Delta H = 30$ Oe, and it absorbed 3 dB of power at the FMR ($f_0 = 40.1$ GHz; average power $P(f_0) = 35$ mW). The resonance characteristic for this transducer is shown in Figure 5, together with that for the UFR-HET. The conversion coefficient for the transducer UFR-CT is 1.2 V/W, two times greater than that of the transducer UFR-HET. The minimum measured signal was about $1 \mu\text{W}$. The shortcoming of the transducer UFR-CT is the presence of a “pedestal” at the level of 5–10 mV, as is shown in Figure 5. This “pedestal” is due to the off-resonance heating of the semiconductor element directly from the mm-wave signal power, and it can be removed by calibration in the off-resonance

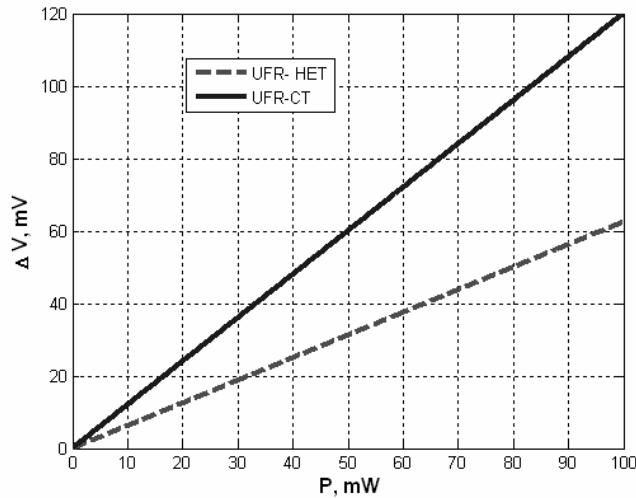


Figure 7. Experimental Volt-Watt characteristics for UFR-semiconductor element structures.

regime. The further improvement of the transducer is related to using a semiconductor element with a higher thermosensitivity. The linear volt-watt characteristics of the transducers with two Hall-elements and the chip transistor are shown in Figure 7.

4. CONCLUSIONS

The systems containing a high-Q uniaxial hexagonal ferrite resonator in the direct contact with a Hall-effect transducer (HET), or any other thermosensitive semiconductor element, allow for frequency-selective measuring of mm-wave power parameters in a wide frequency range.

The possible physical mechanisms of a useful voltage, proportional to the input microwave power, induced in a HET are analyzed.

An analytical model for this useful voltage detected by the system UFR-HET has been developed. The power absorbed by the UFR is derived as a function of the physical parameters of the UFR and its coupling with a transmission line (waveguide), where it is placed in the general multimode case. The thermal balance equation in the system is composed, and the solution of the corresponding Cauchy problem yields the temperature increase in the system that is proportional to the useful voltage.

It is shown that the most probable effect leading to the useful converted voltage is the Nernst-Ettingshausen effect in a semiconductor

element, while frequency selectivity is provided by a ferrite resonator.

To increase sensitivity and conversion coefficients of a transducer based on the described schematic, it is necessary to use an HET with a higher thermal coefficient of voltage, assure the best possible heat contact between the ferrite resonator and the semiconductor element (increase the surface of their contact, for example, using a disk ferrite resonator), and employ a highly sensitive microvoltmeter to register converted signals of low intensity.

ACKNOWLEDGMENT

The results presented in this work were mainly obtained in the Ferrite Laboratory of Moscow Power Engineering Institute (Technical University), where the first author worked before joining the University of Missouri-Rolla.

REFERENCES

1. Kitaytsev, A. A. and M. Y. Koledintseva, "Physical and technical bases of using ferromagnetic resonance in hexagonal ferrites for electromagnetic compatibility problems," *IEEE Trans. Electromag. Compat.*, Vol. 41, No. 1, 15–21, Feb. 1999.
2. Koledintseva, M. Y., A. A. Kitaitsev, V. A. Konkin, and V. F. Radchenko, "Spectrum visualization and measurement of power parameters of microwave wide-band noise," *IEEE Trans. Instrum. Measur.*, Vol. 53, No. 4, 1119–1124, Aug. 2004.
3. Koledintseva, M. Y., "Modulation of mm-waves by an acoustically controlled monocrystalline hexagonal ferrite resonator," *Journal of Electromagnetic Waves and Applications*, Vol. 20, No. 1, 127–133, Jan. 2006.
4. Bogdanov, G. B., "Theory of inertial nonlinear phenomena in ferrites at microwaves," *Physical and Physico-Chemical Properties of Ferrites*, 297–309, Minsk, 1966 (in Russian).
5. Koledintseva, M. Y., "Frequency-selective power transducers, "Hexagonal ferrite resonator — semiconductor element," *Proc. Progress in Electromagnetic Research Symposium (PIERS 2006 Cambridge)*, 241–245, Cambridge, MA, USA, March 26–29, 2006.
6. Kuchis, E. V., *Methods for Investigation of the Hall-effect*, *Sov. Radio*, Moscow, 1974 (in Russian).
7. Ibrahiem, A., C. Dale, W. Tabbara, and J. Wiart, "Analysis of the temperature increase linked to the power induced by RF source," *Progress In Electromagnetics Research*, PIER 52, 23–46, 2005.

8. Haala, J. and W. Wiesbeck, "Modeling microwave and hybrid heating processes including heat radiation effects," *IEEE Trans. Microwave Theory and Techniques*, Vol. 50, No. 5, 1346–1354, May 2002.
9. Gurevich, A. G., "Ferrite ellipsoid in a waveguide," *Radiotekhnika i Elektronika (Radio Engineering and Electronics)*, No. 8, 780–790, 1963 (in Russian).
10. Gurevich, A. G. and G. A. Melkov, *Magnetization Oscillations and Waves*, CRC Press, Boca Raton, FL, 1996.
11. Koledintseva, M. Y., "Electromagnetic modeling of 3D periodic structure containing magnetized or polarized ellipsoids," *Opto-Electronics Review*, Vol. 14, No. 3, 253–262, 2006.
12. Vainshtein, L. A., *Electromagnetic Waves, Moscow, Radio i Svyaz (Radio and Telecommunication)*, 1988 (in Russian).
13. Koledintseva, M. Y. and A. A. Kitaitsev "Modulation of millimeter waves by acoustically controlled hexagonal ferrite resonator," *IEEE Trans. Magn.*, Vol. 41, No. 8, 2368–2376, August 2005.
14. Sihvola, A., *Electromagnetic Mixing Formulas and Applications*, IEEE Electromagnetic Wave Series 47, Section 4.2.1, 63–66, 1999.
15. Koledintseva, M. Y., S. K. R. Chandra, R. E. Dubroff, and R. W. Schwartz, "Modeling of dielectric mixtures containing conducting inclusions with statistically distributed aspect ratio," *Progress In Electromagnetics Research*, PIER 66, 213–228, 2006.